Ventricular-Vascular Coupling in the Pulmonary Circulation

5

Nicholas E. Hobson and Kendall S. Hunter

Abstract

Ventricular performance quantities such as the end-systolic pressure-volume relationship (ESPVR) have been the subject of numerous basic science studies, yet their clinical use remains limited, particularly in the right ventricle (RV). This is primarily due to the difficulty of volume measurements in the small, crescent-shaped RV via catheterization. However, such parameters should be a superior indicator of ventricular function compared with other hemodynamic measures used in the prognosis of pulmonary arterial hypertension (PAH), such as pulmonary vascular resistance index (PVRI). Thus, there is clinical interest in methods that estimate ESPVR and related parameters while being minimally invasive. The focus of this chapter is on one such method and its possible non-invasive extensions, a modified single-beat method which estimates the ventricular-vascular coupling ratio (VVCR), or the ratio of end-systolic ventricular elastance (E_{es}) to arterial elastance (E_a). Within the single-beat elastance framework, the maximum isovolumic pressure ($P_{max,iso}$) and end-systolic pressure are found; based on a novel assumption about the slopes of E_{es} and E_a, VVCR is then computed using only pressure. A lower coupling ratio is hypothesized to be a good indicator of RV dysfunction and failure, as represented by the World Health Organization Functional Class (WHO-FC). We also investigate two non-invasive forms of this method using measurements in children: one in which pressure data is obtained from the velocity of the tricuspid regurgitant (TR) jet measured by Doppler ultrasound; and another in which myocardial performance index (MPI) is

N.E. Hobson • K.S. Hunter (✉)
Department of Bioengineering, University of Colorado Anschutz Medical Campus, Aurora, CO 80045, USA
e-mail: nicholas.hobson@ucdenver.edu; kendall.hunter@ucdenver.edu

M.K. Friedberg, A.N. Redington (eds.), *Right Ventricular Physiology, Adaptation and Failure in Congenital and Acquired Heart Disease*, https://doi.org/10.1007/978-3-319-67096-6_5

used to approximate VVCR. Finally, a very new but existing noninvasive method to compute VVCR using only volumes is explored as a predictor of reactivity in children with PH.

Keywords
Ventricular-vascular coupling • Pulmonary circulation

Introduction

Ventricular performance quantities such as the end-systolic pressure-volume relationship (ESPVR) have been the subject of numerous basic science studies, yet their clinical use remains limited, particularly in the right ventricle (RV). This is primarily due to the difficulty of volume measurements in the small, crescent-shaped RV via catheterization. However, such parameters should be a superior indicator of ventricular function compared with other hemodynamic measures used in the prognosis of pulmonary arterial hypertension (PAH), such as pulmonary vascular resistance index (PVRI). Thus, there is clinical interest in methods that estimate ESPVR and related parameters while being minimally invasive.

The focus of this chapter is on one such method and its possible non-invasive extensions, a modified single-beat method, which estimates the ventricular-vascular coupling ratio (VVCR), or the ratio of end-systolic ventricular elastance (E_{es}) to arterial elastance (E_a). Within the single-beat elastance framework, the maximum isovolumic pressure ($P_{max,iso}$) and end-systolic pressure are found; based on a novel assumption about the slopes of E_{es} and E_a, VVCR is then computed using only pressure. A lower coupling ratio is hypothesized to be a good indicator of RV dysfunction and failure, as represented by the World Health Organization Functional Class (WHO-FC). We also investigate two non-invasive forms of this method using measurements in children: one in which pressure data is obtained from the velocity of the tricuspid regurgitant (TR) jet measured by Doppler ultrasound; and another in which myocardial performance index (MPI) is used to approximate VVCR. Finally, a very new but existing noninvasive method to compute VVCR using only volumes is explored as a predictor of reactivity in children with PH.

Concepts and Background

Characterization of the pressure-volume relationship of the heart as a pump dates back to an 1898 paper by Otto Frank [1], in which he presented a P-V diagram of contractions of the isolated frog left ventricle. Frank made two important observations about this diagram: first, peak systolic activity, whether measured by isovolumic pressure or isobaric ejection volume, is related to preloaded end-diastolic volume (EDV); and second, when the ventricle is in ejecting mode, the curve produced by connecting the end-systolic points of different PV loops (known as the end-systolic pressure-volume relationship, or ESPVR) is quite different than the isovolumic (non-ejecting) curve. These observations were well-received in Europe, and in 1914 Ernest Starling published a series of papers that led to the now well-known Frank-Starling law of the heart [1, 2], which describes the ability of the heart to compensate for varying end-diastolic volumes by varying its work output accordingly.

Research on this topic waned until the 1950s, when interest in pressure-volume relationships of the heart experienced a resurgence. Studies by Ullrich et al (1954), Hild and Sick (1955), and Hild and Herz (1956) obtained pressure-volume relationships for mammalian hearts, which proved to be somewhat different than the previous studies using the frog ventricle. These studies revealed the ESPVR displayed only slight curvilinearity within physiologic pressure ranges. Monroe et al. (1960, 1961, 1964) showed similarly that the ESPVR for the dog ventricle under

the control condition was almost linear, contrary to studies of the frog that showed strong dependence of ESPVR on preload and afterload history.

The ESPVR Relationship and Elastance

The near-linearity of the ESPVR curve has been validated in both the left ventricle (Cross et al. 1961, Taylor et al. 1969) and right ventricle (Lafontant et al. 1962). Perhaps the most substantial work on the characterization of ESPVR and PV relationships of the left ventricle come from the 1970's to 1980's in Japan from authors Suga, Sagawa, and Sunagawa. These serial works on the in vivo canine heart further confirmed and refined the linearity of ESPVR in the physiologic range and helped advance understanding of a wide array of other properties of these measurements. Advances in catheter technology and the advent of the conductance catheter allowed instantaneous volume measurements of the left ventricle in vivo [3], meaning ESPVR could be obtained in a cardiac catheter lab by altering preload (EDV) and obtaining a series of PV loops and connecting their end-systolic points (Fig. 5.1). As the end-diastolic volume increases and the loops shift to the right, end-systolic pressure increases along the ESPVR line up to a maximum pressure for isovolumic contraction [4]. Because ESPVR is relatively insensitive to changes in preload, afterload, and heart rate, it provides a valuable index of systolic cardiac function. Specifically, the slope of the ESPVR is a measure of end-systolic elastance (E_{es}) of the ventricle. Furthermore, a second useful measure, effective arterial elastance (E_a), can be obtained as the slope of the line from the pressure-volume loop, from the end-systolic PV point (upper-left of the PV box) to the end-diastolic volume intercept (bottom-right). Arterial elastance was defined as the ratio of end-systolic pressure to stroke volume, P_{es}/SV (Fig. 5.1). This definition, from a 1983 work by Sunagawa and colleagues examining LV-arterial interaction, is based on the assumption that vascular impedance can be modeled as a three-element Windkessel model [5]. By defining SV in terms of mean arterial flow over a single cardiac cycle, the P_{es}-SV relationship in the arteries was described analytically

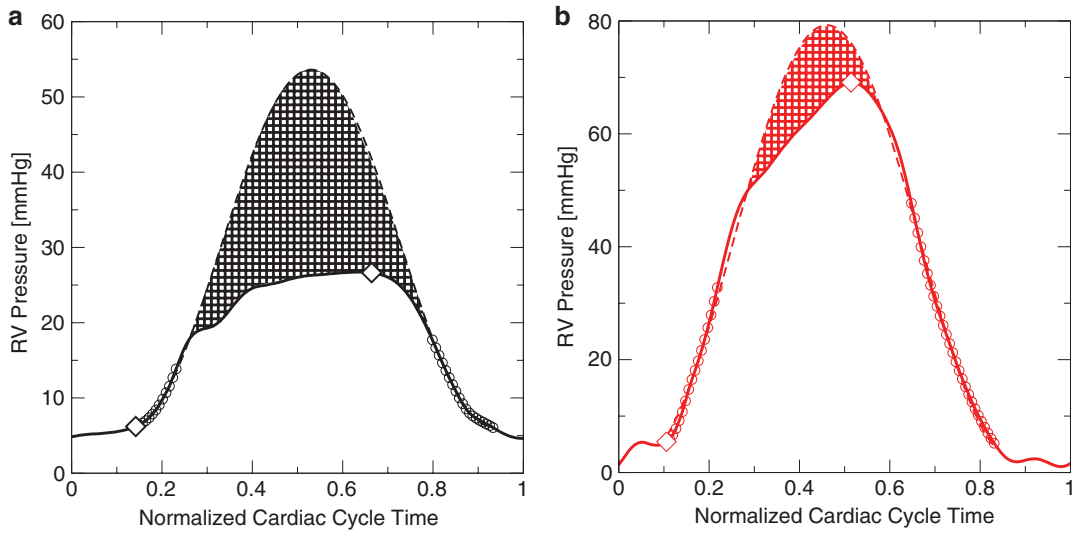

Fig. 5.1 (**a**, **b**) Estimation of VVCR using the pressure only method. A WHO FC 1 patient (*left plot*) has a significantly smaller pressure ejection requirement (i.e. max RVSP, shown as *diamonds* near *end-systole*) than maximum isovolumic pressure, yielding high VVCR-P, while the WHO FC 4 patient (*right plot*) has little "overhead" between these two quantities, yielding low VVCR-P

as a linear relationship when characteristic arterial impedance, peripheral resistance, compliance, and systolic and diastolic durations are constant. The expression describing the slope of that relationship involving those arterial parameters was denoted by E_a (effective arterial elastance). Because both E_{es} and E_a are given in the same units, their ratio can be computed as E_{es}/E_a to provide a measure of ventricular-vascular coupling.

Arterial Elastance and Ventricular-Vascular Coupling

Works by Sunagawa et al. [5, 6] sought to test the hypothesis that ventricular external work would be maximized if the ventricular and arterial elastances are equal. They investigated the optimal arterial resistance under a number of variable parameters such as end-diastolic volume, contractility, heart rate, and arterial compliance, and found that optimal arterial resistance varied only slightly with arterial compliance, while varying widely with contractility and heart rate. These findings suggest that the ratio of ventricular and arterial elastance is optimally nearly unity, which gives rise to the idea that the ventricle and vasculature are coupled from an energetics viewpoint. In other words, optimal flow (and optimal energy transfer from the ventricle through the vasculature) is achieved at an arterial elastance equal to ventricular elastance. Thus, the effects of increased afterload on PV loops and ESPVR should be significant.

Single-Beat Methodology

In 1991, Takeuchi et al. proposed a novel method for the calculation of the slope of the ESPVR (E_{es}) using a single beat [7]. They realized that the maximum pressure the ventricle can produce during isovolumic contraction could be estimated from the pressure trace alone, and the slope of the ESPVR could be obtained by drawing a line from this point tangential to the upper-left corner of a single PV loop (i.e. near the end-systolic point). Sinusoidal curve fitting is performed on the pressure trace of the ventricle using data points which correspond to periods of isovolumic contraction and relaxation in order to estimate P_{max}. This is a much easier method than the previous one for generating the ESPVR, which involved creating at least three PV loops by altering the end-diastolic volume.

This method has also been validated for the right ventricle by Brimioulle et al. in 2003 [8]. A number of assumptions and limitations unique to the RV were addressed in their work. The triangular shape of typical PV loops in the RV means that end-systole and end-ejection often occur at different times. The upper-left corner was used as the end-systolic point, which is valid for the LV but less so for the RV. The assumption that isovolumic beats are sinusoidal, established by Sunagawa by Fourier analysis for the LV, was verified by comparing estimated $P_{max,iso}$ of ejecting beats with observed P_{max} for isovolumic beats of the same starting EDV, which were found to be strongly correlated. Due to the challenges of measuring RV volume in vivo, they determined RV volume changes by integrating flow measured in the proximal pulmonary artery with a widely validated ultrasonic method. They also found expected changes in E_{es} and E_a under a variety of inotropic states.

Pulmonary Hypertension

Pulmonary hypertension was first classified in 1973 in a meeting organized by the World Health Organization. PH is defined as a hemodynamic and pathological condition in which a mean pulmonary arterial pressure (PAP) of 25 mmHg or greater at rest is measured by right heart catheterization. Normal PAP is 14 ± 3 mmHg with an upper limit of about 20 mmHg. The significance of a mean PAP of 21–24 mmHg is unclear [9].

The clinical classification of PH has undergone some changes in international conferences since the initial 1973 WHO classification, but the basic differentiation of primary and secondary PH is still apparent. The broad categories of the classification agreed upon at the fourth World

Symposium for PH at Dana Point, California in 2008 [9] are as follows:

1. Pulmonary arterial hypertension (PAH)
2. Pulmonary veno-occlusive disease and/or pulmonary capillary haemangiomatosis
3. Pulmonary hypertension due to left heart disease
4. Pulmonary hypertension due to lung diseases and/or hypoxia
5. Chronic thromboembolic pulmonary hypertension
6. PH with unclear or multifactorial mechanisms

The focus of the methods discussed in this chapter is primary hypertension (group 1, PAH), or PH not caused by other health problems.

Diagnosis

Diagnosis of PH is a process of exclusion, so often different diagnostic tools and methods need to be employed to eliminate all other possible causes. In the case of PAH, this means ruling out left heart disease, veno-occlusive disease, lung disease, and chronic thromboembolism [10].

Symptoms of PAH are often mild and present mainly during exercise, and can include shortness of breath, fatigue, weakness, angina, syncope, and abdominal distension. Auscultory physical signs that may aide diagnosis are: tricuspid valve regurgitation murmur, a diastolic murmur of pulmonary insufficiency, and an RV third heart sound. Patients with advanced disease may present with signs such as ascites, peripheral edema, and cool extremities [10]. However, these physical signs vary widely and may not present at all.

Echocardiography can provide an estimation of PAP by obtaining velocity measurements of regurgitant tricuspid valve jets, which occur in more than 70% of patients with PAH [11] Velocity of TR jets is measured using Doppler ultrasound. By using a simplified form of Bernoulli's equation, mean PAP can be calculated as $4 \times (\textit{tricuspid regurgitant velocity})^2 + (\textit{estimated right atrial pressure})$. However, echocardiography is limited by the noise inherent in ultrasound imaging, which can lead to faint or inaccurate signals.

The gold standard for the diagnosis of PAH is right heart catheterization (RHC), and it is necessary for confirming such a diagnosis [10]. The following variables must be obtained: PAP, right atrial pressure, RV pressure, pulmonary wedge pressure (PWP), and cardiac output (CO) by either thermodilution or the Fick method. A mean PAP of 25 mmHg or greater with a PWP of 15 mmHg or less in the absence of other causes confirms a diagnosis of PAH [10]. Although RHC is a relatively safe procedure, it is invasive, and therefore carries some risk to the patient.

Assessment of RV function

A number of methods for the assessment of RV function have been proposed and validated over the past 30 years, varying widely in invasiveness as well as efficacy and accuracy. In 1984, Kimchi et al. became the first group to evaluate RV ejection fraction (RVEF) using radionuclide ventriculography [12]. They defined RV failure as RVEF less than 38%. In 1989, Vincent et al. obtained RVEF using a modified PA catheter with a fast-response thermistor, utilizing the thermodilution method [13]. However, these methods are not ideal both because they are either nuclear or invasive, and because RVEF varies widely in normal patients from 30% to 60%.

Cardiac magnetic resonance (CMR) imaging is the gold standard for evaluating RV function and can reliably quantify RV volume and RVEF. Delayed contrast-enhanced CMR has also been shown to detect fibrotic tissue in the RV wall, but can only detect regional changes in myocardial tissue. Contrast-enhanced T1-weighted CMR allows the detection of diffuse fibrosis [14]. However, CMR is expensive and availability is often limited.

Echocardiography is currently the most practical tool for assessing RV function at the bedside. A failed right ventricle is severely dilated, which can be assessed by comparing the area of the chamber with that of the left ventricle. A ratio of RV:LV area less than 0.6 is considered normal,

and greater than 1 is considered failing [10]. In 1995, Masahiro, et al. demonstrated the efficacy of an automated method for obtaining a correlate of the ESPVR based on the area of the chamber from echocardiography, rather than volume measured by catheterization [15]. They showed that the ESPAR responded similarly to ESPVR as RV function declined. Another sign readable from echocardiography is paradoxical septal motion during systole, which indicates RV systolic pressure overload. In Doppler mode, the ejection flow can show pulmonary hypertension by a shortening of the acceleration time of flow (<100 ms). A related parameter proposed by Tei et al. in 1995 takes the ratio of combined isovolumic contraction and relaxation times compared with ejection time, termed the myocardial performance index (MPI) [16]. Longer periods of isovolumic contraction and relaxation yield a higher MPI, and indicate worse RV function. Interestingly, this measure bears a certain similarity to VVCR, because longer isovolumic periods will inevitably yield lower estimated maximum isovolumic pressures.

Advances in 3D echocardiography in the past years have made the non-invasive measurement of RV volume possible. There are several methods for calculating RV volumes from echocardiographic images. One involves the manual tracking of RV area through a series of slices, while the other uses border-detection algorithms to automate this process. These measurements have been shown to correlate well with volume measurements obtained from CMR, but consistently predict volumes 20–34% smaller than those obtained by CMR [14]. Thus, 3D echocardiography requires further refinement and validation, but could become a gold standard in the future.

Mechanical-Mechanistic Links

Despite its origin in the pulmonary vasculature, the proximate cause of death in pulmonary hypertension is often RV failure [17]. In response to pulmonary hypertension, the RV undergoes hypertrophic remodeling reflecting increased myocyte size and altered programs of gene expression. Ultimately this pathologic remodeling leads to wall thinning, chamber dilation, and RV failure [18]; however, therapies that directly target the dysfunctional RV are not currently available [10, 19]. Inflammatory processes in the pulmonary vasculature are increasingly recognized to play a role in the progression of pulmonary hypertension [20], and additional evidence suggests that inflammatory-fibrotic modeling contributes importantly to the progression of heart failure [21]. Together, these observations suggest the need to examine the relationships between RV overload and function, hypertrophic remodeling, and activation of inflammatory-fibrotic processes in the RV, in the setting of pulmonary hypertension.

Animal and Clinical PV Studies

Animal Work

A significant amount of work has been done in recent years to better characterize the role of ventricular adaptation to pulmonary hypertension in animal models. A 2004 interspecies study by Wauthy et al. [22] showed that while E_{es} and E_a both increased during short (10 min) bouts of hypoxia-induced hypertension, VVCR remained optimal in dogs, goats, and pigs. This trend was also observed in induced embolism and proximal pulmonary artery constriction in dogs. In all cases, a proportional increase in E_{es} compensated for elevated E_a, and optimal coupling was maintained.

In a 2007 study by Grignola et al. [23] of an acute PH model in 6 anesthetized sheep in which proximal occlusion and whole-pulmonary vasoconstriction (by phenylephrine) were compared, coupling, as assessed by an energy transmission ratio and the ratio of pulsatile energy to total energy, was better maintained in the vasoconstictive model. Their model showed that activation of smooth muscle cells in the main pulmonary artery helped maintain energy transfer from the RV to the hypertensive pulmonary vasculature by preserving the reflected wave magnitude.

Several models of progressive pressure overload ("chronic" PAH) have shown that the RV in healthy animals operates close to maximum efficiency (VVCR ≈ 2), decreases as afterload increases to operate close to the point of maximal stroke work (VVCR ≈ 1), and finally decouples (VVCR <1) approaching failure. The trend is one of continually increasing E_a, with E_{es} initially increasing and finally returning to baseline values. This was shown in a porcine model by Ghuysen et al. [24] of progressive pulmonary embolism by injection of blood clots. E_a increased continually with each injection, while E_{es} increased after the first two injections, but failed to increase further. Thus, E_{es}/E_a initially decreased to values near optimal stroke work, but the final injection caused values to drop below 1, decreased stroke work, and RV dilation.

Another animal model of interest is a 2007 study by Missant et al. [25] regarding the effects of Levosimendan on RV dysfunction in a porcine model. Levosimendan is a calcium sensitizer—it increases the sensitivity of the heart to calcium, thus increasing cardiac contractility without a rise in intracellular calcium. Levosimendan exerts its positive inotropic effect by increasing calcium sensitivity of myocytes by binding to cardiac troponin C in a calcium-dependent manner. In healthy animals, Levosimendan improved contractility but actually reduced efficiency (i.e. VVCR dropped slightly), with no change in PVR or characteristic impedance. The lack of improvement in efficiency was explained as the RV was already operating at max efficiency (best coupling) in health. In an ischemia/reperfusion model of RV failure along with pressure overload (PA banding), Levosimendan increased inotropy (i.e. E_{es}), thus maintaining or improving coupling.

Finally, a study by Kind et al. sought to better characterize the isovolumic beat in rats using Fourier analysis. They induced stable and progressive acute pulmonary hypertension in the rats by the administration of monocrotaline 40 and 60 mg/kg, respectively. Isovolumic beats were obtained by clamping the pulmonary artery in these rats and controls. The waveforms were then normalized in pressure and time, averaged, and modeled by a Fourier series using six harmonics. This normalized waveform was parameterized and used for curve fitting of single beats, then compared to other isovolumic beat models from the literature, including the sinusoidal method by Sunagawa et al. mentioned earlier in this chapter. It was found that the Fourier-based model was more accurate than the other models at predicting maximum isovolumic pressure from ejecting beats (compared with true isovolumic beats obtained by pulmonary artery clamping during the prior beat), and that the other models generally underestimated maximum isovolumic pressure. This approach holds great promise in improving single-beat methodology in humans.

Clinical Work

Although there has been much work done in the lab characterizing the pressure-volume relationship of the ventricle, and though these works generally strive to emphasize the potential clinical usefulness of PV loops, their use in clinical settings has remained extremely limited for a number of reasons. First, the procedures for obtaining instantaneous pressure and volume measurements require invasive catheterization, optimally with high-fidelity catheters. Techniques for volume measurements in particular have been difficult and imprecise. Measurements of volume of the RV are especially troublesome due to its location, smaller size, and non-uniform geometry. Furthermore, many clinical decisions can be made based on more easily-obtained measures, such as ejection fraction [26].

However, there have emerged a number of clinical studies in recent years demonstrating and validating the usefulness of PV-loop-derived parameters. A study in 1992 by Kelly et al. [27] tested the use of effective arterial elastance of the LV as an index of vascular load in normal and hypertensive humans. The study found that E_a based on PV loops was nearly identical to E_a derived from a three-element Windkessel model for normal patients, and that it exceeded simple resistance by nearly 25% in hypertensive patients, due to decreased compliance and wave reflection. The findings suggest that even E_a alone, not to

speak of full ESPVR or E_{es}/E_a coupling, could provide a convenient assessment of arterial impedance and its effects on ventricular function in hypertensive patients.

The earliest population-based study assessing diagnostic capabilities of LV PV loops comes from Lam et al. from Minnesota in 2007 [28]. This study compared patients exhibiting heart failure with a normal ejection fraction (HFnlEF) with patients with hypertension but no heart failure (HTN), and with patients without cardiovascular disease. The authors characterized left ventricular volume, effective arterial elastance, LV end-systolic elastance, and LVdiastolic elastance and relaxation noninvasively. Their results showed increased E_{es} for hypertensive and HFnlEF patients compared with the control, as well as a shift to the right of the V_0 volume intercept for HFnlEF patients relative to HTN patients, indicating an overall increase in ventricular volume. They observed similar differences in the EDPVR curves for the three groups, with hypertensive patients having a greater EDV than HFnlEF patients. Their work showed a probable role of diastolic dysfunction in HFnlEF patients relative to HTN patients. Furthermore, it shows the potential diagnostic power of ESPVR and EDPVR curves for distinguishing specific cardiovascular disorders.

Furthermore, a 2004 study by Kuehne et al. validated the single-beat method for the RV using cine MRI to obtain RV volume, and also undertook a small clinical study comparing 6 control patients to 6 patients with chronic pulmonary hypertension. They obtained indexes of cardiac pump function, measured as cardiac index or the ratio of cardiac output to body surface area, E_{es} indexed to myocardial mass and ventricular-arterial coupling (E_{es}/E_a). In patients with PAH, RV pump function was decreased, myocardial contractility was enhanced, and VVC was inefficient compared with the control group. These results agree with the expected physiologic impact of PAH on RV function discussed above, and are encouraging for the minimally-invasive prognosis of PAH. Finally, a recent study by Sanz et al. [29] used a different simplification of the single-beat method to use MRI combined with invasive measurement of mPAP to approximate the inverse of VVCR (e.g. E_a/E_{es}) in 143 adults with PH. Their E_a and VVCR both showed increasing group trends when sub-divided by increasing quartiles of PVRI. Unfortunately, their approximation was quickly shown to be incomparable to the gold-standard in that it neglects the zero-pressure intercept of RV volume [30]. This however does not mean that their approximation lacks clinical utility; indeed we show in our work below that this measure clearly distinguishes reactive vs. unreactive children with PAH in terms of their response to pulmonary vascular vasodilators.

Emerging Methods for Assessment of VVCR

It is useful to distinguish between patients with early- and late-stage pulmonary hypertension as "compensated" and "failing," in terms of ventricular function. In early-stage PAH, as the ventricle must overcome greater vascular pressure and impedance, the end-systolic pressure will increase to compensate, which is achieved by an increase in ventricular elastance. This progression will also be reflected in a slightly increased E_a as distal vessels dilate, leading to increased mPAP; and as vascular remodeling gradually stiffens the arterial vasculature, leading to increased pulse pressure. Together these lead to a greater P_{es}. Thus, the coupling ratio between the ventricle and arteries, E_{es}/E_a, may decrease somewhat but should remain above or close to unity. Over time however, the heart becomes overworked, and P_{es} approaches the maximum isovolumic pressure the ventricle can produce, as shown in Fig. 5.1a, b. A patient transitions from compensated to failing when the ventricle and vasculature become uncoupled, and the ventricle begins to dilate to meet cardiac output needs. The PV loop shifts to the right and becomes narrower as end-diastolic volume increases and stroke volume decreases [31–34]. These patients should have a markedly decreased coupling ratio, which signifies uncoupling of the ventricle and vasculature. We have preliminary evidence below that

these patients are unreactive to pulmonary vasodilators in terms of cardiac output, indicating that lack of reactivity in PVR is as suggestive of problems with RV function as much as problems in vascular function.

Invasive Pressure-Only VVCR

The basis for this work is a modification of the single-beat method that estimates VVCR while eliminating the need for volume measurement. Re-examining Fig. 5.1a, it can be seen that:

$$E_{es} \cong \frac{P_{\max,iso} - P_{es}}{SV} \tag{1}$$

and given the definition [6, 27].

$$E_a = \frac{P_{es}}{SV} \tag{2}$$

Inserting Eqs. (1) and (2) into the expression for VVCR, we have:

$$\frac{E_{es}}{E_a} \cong \frac{P_{\max,iso} - P_{es}}{SV} \cdot \frac{SV}{P_{es}} = \frac{P_{\max,iso} - P_{es}}{P_{es}} = \frac{P_{\max,iso}}{P_{es}} - 1 \tag{3}$$

Thus, from Eq. (3) we obtain an expression for VVCR as a simple ratio of maximum isovolumic pressure to end-systolic pressure. The single-beat method can be applied to pressure traces from the RV, estimating $P_{max,iso}$ by sinusoidal curve fitting to periods of isovolumic contraction and relaxation, and comparing this value to the observed end-systolic pressure to obtain an estimate of VVCR.

Based on the above analysis, the coupling ratio E_{es}/E_a actually quantifies the heart's "reserve" capacity, or the ratio of its maximum pressure capability to its current pressure requirement, at a particular inotropic state. As such, we hypothesize that this ratio will be prognostic of RV failure in PH. Our approach computes the ratio using only pressure, allowing us to avoid having to acquire more difficult, less readily available PV loops. By using only clinically feasible standard-of-care measurements, we enable wider clinical applicability of the resulting prognostic, and further open the possibility of non-invasive estimation of the coupling ratio. Our simplified approach promises to enable more routine assessment of RV function. Furthermore, our quantitative approach of describing the system has the potential to better guide future basic science and mechanistic studies of the disease as well as assist in the interpretation of future therapeutic study results.

Pressure Data Analysis

All data analysis was performed in MATLAB. Pressure traces from the right ventricle were divided into single beats by ECG gating. $P_{max,iso}$ was determined by fitting the equation $P = a + b \cdot \sin(c \cdot t + d)$, [8] where P is pressure and t is time, to pressure values from the end-diastolic point up to the point of the maximal value of the first derivative, corresponding to isovolumic contraction, and from the time of the minimal value of the first derivative to the same pressure value as the end-diastolic point, corresponding to isovolumic relaxation. The end-diastolic point was defined as the time at which dP/dt exceeds 200 mmHg/s [7]. Curve fitting was performed using the Levenberg-Marquardt algorithm for non-linear least squares [8].

The coupling ratio E_{es}/E_a was determined from Eq. (3), which required an additional assumption regarding the timing of end-systole. Alyono et al. [31] found that 30 ms before dP/dt_{min} is the best definition for end-systole using pressure data alone, compared with definitions using pressure and volume together. Because the pressure data was obtained with a sampling frequency of 250 Hz, data points were separated by 4 ms, so end-systole was defined as 32 ms, or 8 data points, prior to dP/dt_{min} rather than 30 ms prior. VVCR was also calculated using P_{max} for a given pulse as end-systole in addition to the 32 ms prior to dP/dt_{min} definition for end-systole, and each method was compared. VVCR (P_{max}) was superior to VVCR (P_{es}) for all tests, so results will only be shown for VVCR (P_{max}).

Initial Results for New Techniques

Indirect evidence that VVCR is related to the progression of right heart remodeling processes can be found by comparing it, as well as load parameters such as mPAP, to tissue markers of hypertrophy, inflammation, or fibrosis. Preliminary comparisons were performed with a small set of neonatal male calves (post-natal day 1), exposed to 14 d hypoxia (simulated elevation 4300 m) or ambient atmosphere (Ft. Collins, CO). Hemodynamics were obtained by right heart catheterization via the jugular vein with a solid state catheter to obtain RV and main PA pressures; post study, the RV and LV were excised and Real Time PCR was used to examine gene expression. Although a low-power data set, the results clearly demonstrate (Table 5.1, Fig. 5.2a, b) that gene products reflective of pressure overload of the cardiac myocyte (β-myosin heavy chain (MHC), skeletal α-actin, Brain natriuretic peptide (BNP)) correlated strongly with mean PA pressure, whereas gene products reflective of myocardial inflammation showed greater dependence on VVCR. Further, ECM remodeling gene products also showed equivalent or greater dependence on the coupling ratio rather than developed mPAP. These results suggest that hypertrophic RV remodeling driven by cardiac myocytes is primarily responsive to increasing pulmonary vascular pressure whereas inflammatory and ECM remodeling in the RV are more sensitive to altered mechanical coupling of the cardiopulmonary system, and reinforce the conclusion that RV remodeling encompasses multiple processes responding to non-identical determinants. Thus, understanding and predicting disease progression from the viewpoint of hemodynamics requires a multifactorial approach.

Non-Invasive Methods

We begin by discussing a Doppler ultrasound technique, which makes use of a simplification of Bernoulli's principle in order to approximate RV pressure from the velocity of the regurgitant tricuspid valve (known as a TR jet). This pressure trace is then used to compute VVCR using the single-beat methodology described above. Also noninvasive in nature, two papers have been published that investigate the use of myocardial performance index (MPI, or "Tei index") [32, 33]. The second of these two is particularly interesting; in it, MPI is shown to most strongly correlate to 6 min walk distance, BNP, cardiac index, mPAP, and PVR, better than other echo measures of RV function. Below we present preliminary evidence that MPI is a good predictor of patient outcomes, as well as derive its relationship to VVCR that may explain its predictive power.

TR Jet Technique

Doppler ultrasound data acquired during catheterization was visualized and processed in Matlab. Noise reduction was first applied using the discrete wavelet transform method described

Table 5.1 *R*-squared values characterizing correlations between hemodynamic parameters (mPAP, Coupling Ratio) and tissue markers of myocyte overload, inflammation, and fibrosis ($n = 9$)

Tissue Marker	NPPB (BNP)	ACTA1	MHY7	MCP-1	IL-1b	IL-1RA	TN-C	OPN	COL 1A1	ED-A Fn
mPAP	0.738	0.545	0.581	0.567	0.370	0.413	0.439	0.602	0.247	0.175
VVCR	0.446	0.324	0.242	0.597	0.657	0.506	0.428	0.597	0.700	0.592
Different?	0.140	0.252	0.151	0.458	0.172	0.389	0.487	0.492	0.068	0.100

Generally, mPAP shows best (and most significant) correlation with tissue markers of myocyte overload, while the coupling ratio displays best correlation with inflammation and fibrosis. Only two correlations approached a significant difference

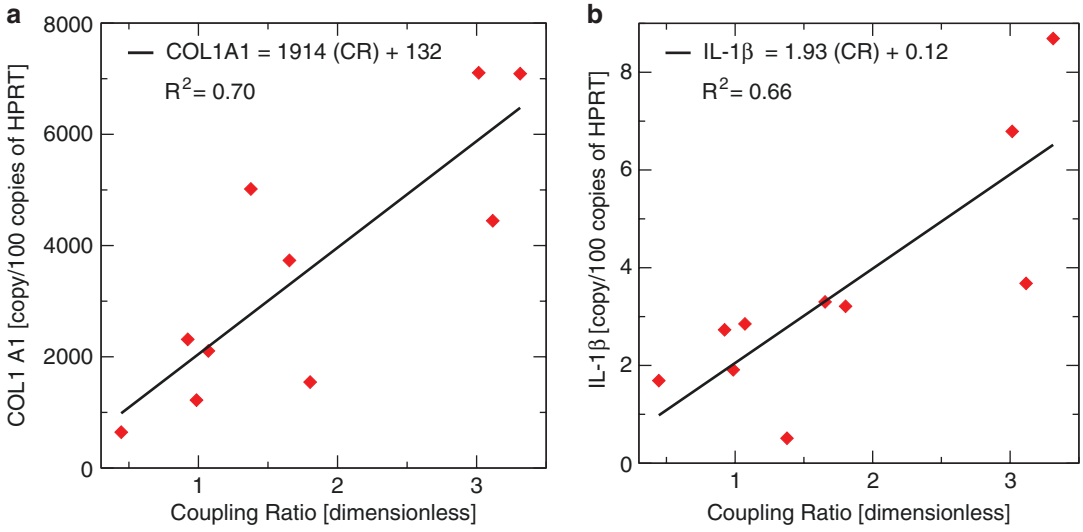

Fig. 5.2 (**a**, **b**) Notable regressions between coupling ratio and inflammatory/fibrotic tissue markers

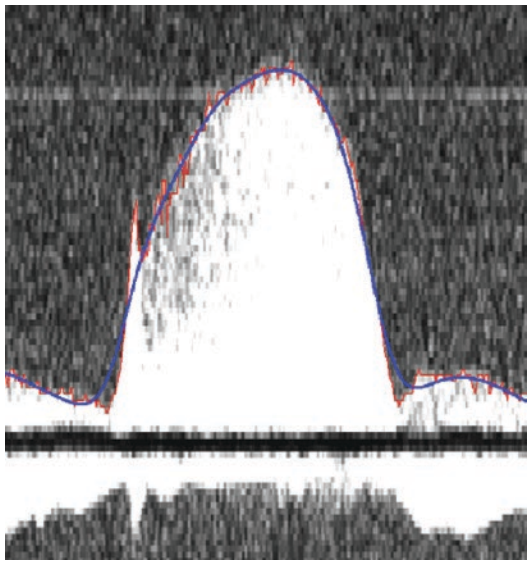

Fig. 5.3 Automatic trace of Doppler US image of TR jet. *Red* raw trace, *Blue* smoothed trace

by Zhang et al. in 2001 [35]. To obtain an envelope of the velocity, traces of the TR jet image were performed by an automatic edge detection routine using an adjustable threshold magnitude. A threshold value was computed automatically based on the noise level, soft thresholding was applied to the detail coefficients, and the image was reconstructed, as shown in Fig. 5.3. The smoothed velocity trace was transformed into approximate right-ventricular pressure by simplification of Bernoulli's principle as $P=4V^2$, as is done in clinical practice, in which P is the ventricular pressure and V is the velocity of the jet. This data was subsequently analyzed again using the techniques described in the Invasive Pressure-Only VVCR section above. Having already performed better in the catheterization cases, the maximal pressure was used in computing the coupling ratio, rather than the end-systolic definition of 30 ms prior to dP/dt_{min}. VVCR was obtained in this fashion for 11 patients, and they follow the same trends (with respect to WHO FC) as with the invasively obtained ratios; however, we have not yet performed outcomes analyses in this small set.

MPI Transformation to VVCR

Given our modeling approach with pressure, we can estimate both P_{es} and $P_{max,iso}$ from merely the isovolumic times and ejection time. These times are routinely collected in our cath lab for the prediction of the myocardial performance index

[MPI—also known as the Tei index [16, 36]], which is computed as $\frac{IVCT + IVRT}{RVET}$, in which IVCT & IVRT are the IsoVolumic Contraction/Relaxation Times, and RVET is the RV Ejection Time. From this time equation, an assumption that P_{es} occurs approximately at the end of ejection time, and the sinusoidal approximation for isovolumic contraction pressure, we can derive the equation.

$$VVCR \approx \cot\left(\pi \frac{MPI}{MPI + 1}\right)^2, \qquad (4)$$

in which π is the constant pi (3.14159…); thus VVCR is approximated by a trigonometric transform of MPI. As MPI varies from low values near zero (indicating good performance) to higher values still less than one (increasing functional limitation), estimated VVCR varies from large values (>5) to values close to zero, predicting the same functional status. To see how well this predicted patient status, we compared MPI, approximated VVCR, and PVRI measured within 48 h in 27 children with PAH to determine how well each predicted WHO FC at follow up, in outcomes categories identical to the three trichotomous groups discussed above. Shown in Fig. 5.4 are box plots of MPI, approximated VVCR, and PVRI for the three outcomes groups (n = 7, 11, 9 for OC1, OC2, OC3, respectively). Clear separation exists in both noninvasive measures between healthy group and severe functional limitation group mean values, whereas due to high variance PVRI has overlap in all three groups. ANOVA showed both noninvasive values differentiated the groups ($p < 0.05$), whereas PVRI did not ($p = 0.08$). Additionally, both noninvasive methods showed better fit to trichotomous and dichotomous WHO-FC based outcomes. While it is currently unclear if the trigonometric transformation of MPI (into VVCR) is advantageous, the transformation does make clear MPI's relation to VVCR; neither have been comprehensively explored as prognostics in pediatric PAH.

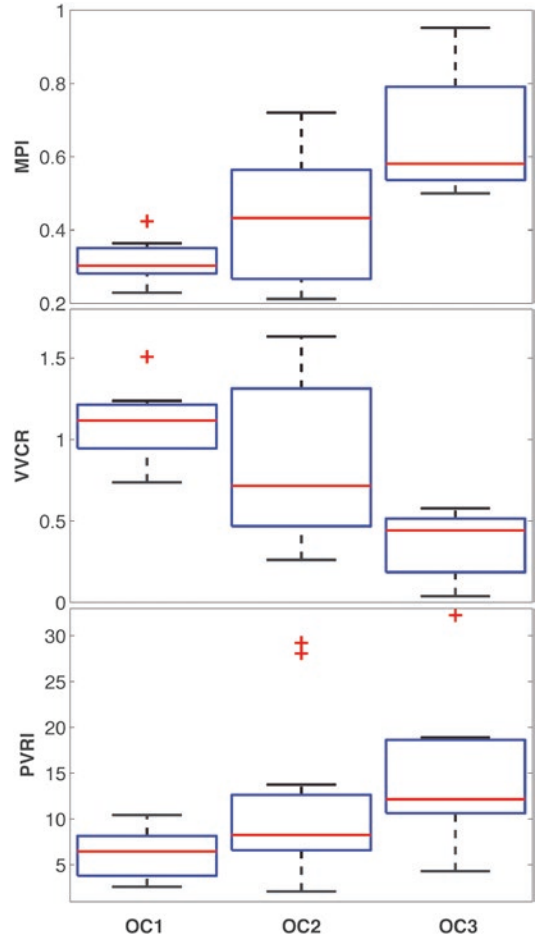

Fig. 5.4 Box plots of MPI, MPI-approximated VVCR, and PVRI. Both noninvasive measures better categorize (and predict) the three WHO FC based outcomes parameters

MRI Technique

As noted above, the Sanz et al. [29] method of computing VVCR, while not comparable to the gold standard, may still possess clinical utility. To explore this possibility, we examined 16 pediatric subjects who underwent MRI and catheterization within month (14 were within 48 h). Age ranged from 3 months to 23 years, with the mean being 11.3 ± 7.4 years. E_a and E_a/E_{max} increased with increasing severity defined by PVR, with $p < 0.001$ for both. E_a/E_{es} steadily increased with increasing PVRI, as might be expected.

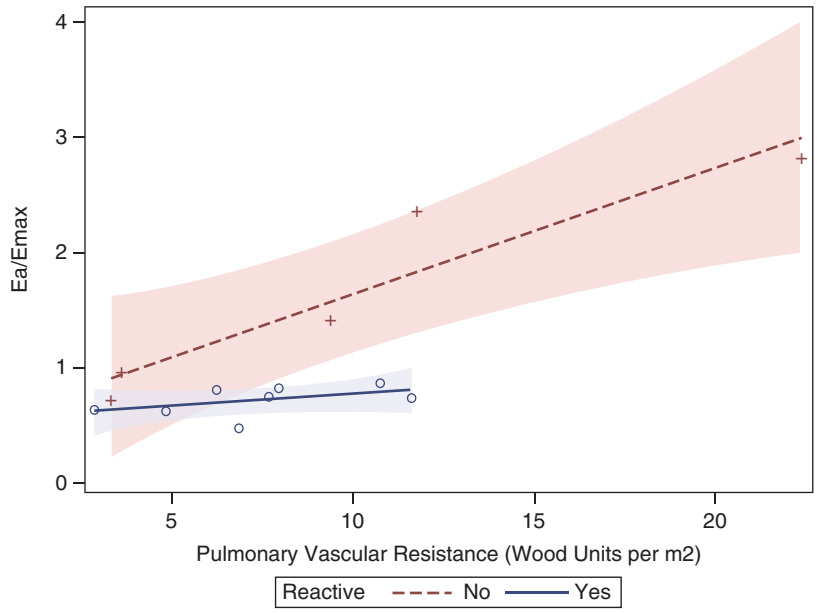

Fig. 5.5 MRI approximated inverse VVCR (with invasive pressure—mPAP), regressed in groups of reactive (*blue*) and non-reactive (*red*) patients vs. PVRI. The sickest patients (with largest inverse VVCR) showed greater decoupling as a function of afterload

Interestingly, patients in the highest quartile were found to be non-reactive to pulmonary vasodilators in PVRI during catheterization. ROC curve analysis determined that an E_a/E_{es} ratio of 0.85 had a sensitivity of 100% and a specificity of 80% of predicting reactivity; further, the AOC of this ROC curve was 0.89 ($p = 0.008$), suggesting quite good discrimination among those who were and were not reactive. Further, preliminary regressions of PVR vs. inverse VVCR in patients grouped by their reactivity in PVR when administered 100% O2 and/or 100% O2 and NO indicated that those unreactive (<20% change) are more uncoupled than those who are reactive (Fig. 5.5). This is in some sense unsurprising, in that PVR reactivity can occur due to reductions in mPAP (vascular reactivity) and increases in cardiac output (RV reactivity).

Limitations

There are a number of limitations associated with the simplified VVCR model. Because VVCR is a ratio of elastances, it can only provide an indirect measurement of ventricular performance as it relates to the state of the vasculature. Thus, parameters involving direct measurement of RV volume, such as ESPVR, will likely always remain better indicators of RV contractility. Furthermore, although the measurement of pressure is much simpler than the measurement of pressure and volume together, our first approximation of VVCR still requires catheterization, meaning it offers no large advantage in terms of invasiveness. Additionally, although it has been shown here to be prognostic, this method for obtaining VVCR requires validation against gold standard measurement. Validation will include pressure-volume studies in both animals and humans, and continual testing should show a strong correlation between VVCR obtained by PV loops and VVCR obtained by pressure alone.

Discussion/Conclusions

Pressure-volume loops and their associated parameters (E_{es}, E_a) are considered the gold-standard measures of ventricular function;

however, the difficult nature of changing ventricular preload and of measuring volume—particularly of the RV—has limited their clinical applicability. Through the 1990s and 2000s a new method—the single beat method—has greatly simplified the process of obtaining PV loops, elastances, and ventricular-vascular coupling ratio. The ratio is a combined measure of contractility and afterload, specifies the efficiency of heart ejection, and is generally a decreasing function of disease worsening. Emerging clinical measurements are providing preliminary evidence that VVCR is a good prognosticator of both left and right-sided heart failure.

By modification of the single beat method equations, we have obtained even simpler and more clinically accessible invasive and noninvasive ways to measure the ventricular-vascular coupling ratio and thereby predict RV function in pediatric PAH. Our invasive data clearly show PVRI and VVCR are independent parameters; thus these VVCR measurements offer new insight into disease progression unavailable from measurements of distal or proximal afterload. Three of the four noninvasive approaches already show high prognostic potential, and all are additionally applicable to adult PH. We conclude that VVCR holds promise for future clinical use in the prognosis of PAH.

References

1. Frank O. Die Grundform des arteriellen Pulses Erste. Z Biol. 1899;37:483–526.
2. Zimmer H. Who discovered the frank-starling mechanism? News Physiol Sci. 2012;17:181–4. https://doi.org/10.1152/nips.01383.2002.
3. Baan J, van der Velde ET, Jong TTA, et al. Continuous stroke volume and cardiac output from intraventricular dimensions obtained with impedance catheter. Cardiovasc Res. 1981;15(6):328–34.
4. Suga H, Sagawa K. Instantaneous pressure-volume relationships and their ratio in the excised, supported canine left ventricle. Circ Res. 1974;35(1):117–26.
5. Sunagawa K, Maughan WL, Burkhoff D, Sagawa K. Left ventricular interaction with arterial load studied in isolated canine ventricle. Am J Phys. 1983;245(5 Pt 1):H773–80.
6. Sunagawa K, Maughan WL, Sagawa K. Optimal arterial resistance for the maximal stroke work studied in isolated canine left ventricle. Circ Res. 1985;56(4):586–95.
7. Takeuchi M, Igarashi Y, Tomimoto S, et al. Single-beat estimation of the slope of the end-systolic pressure-volume relation in the human left ventricle. Circulation. 1991;83(1):202–12.
8. Brimioulle S, January F, Tabima DM, et al. Single-beat estimation of right ventricular end-systolic pressure-volume relationship. Am J Phys. 2003;284(5):H1625–30. https://doi.org/10.1152/ajpheart.01023.2002.
9. Rich S. Primary pulmonary hypertension: executive summary from the World Symposium-Primary Pulmonary Hypertension 1998. Geneva World Health Organization. 1998. http://scholar.google.com/scholar?q=Executive+Summary+from+the+World++Symposium+on+Primary+Pulmonary+Hypertension&btnG=&hl=en&as_sdt=0%2C6##0. Accessed 25 Sept 2013.
10. Galiè N, Hoeper MM, Humbert M, et al. Guidelines for the diagnosis and treatment of pulmonary hypertension: the Task Force for the Diagnosis and Treatment of Pulmonary Hypertension of the European Society of Cardiology (ESC) and the European Respiratory Society (ERS), endorsed by the Internat. Eur Heart J. 2009;30(20):2493–537. https://doi.org/10.1093/eurheartj/ehp297.
11. Yock PG, Popp RL. Noninvasive estimation of right ventricular systolic pressure by Doppler ultrasound in patients with tricuspid regurgitation. Circulation. 1984;70(4):657–62. https://doi.org/10.1161/01.CIR.70.4.657.
12. Kimchi A, Gray Ellrodt A, Berman DS, Riedinger MS, Swan HJC, Murata GH. Right ventricular performance in septic shock: A combined radionuclide and hemodynamic study. J Am Coll Cardiol. 1984;4(5):945–51. https://doi.org/10.1016/S0735-1097(84)80055-8.
13. Vincent JL, Reuse C, Frank N, Contempre B, Kahn RJ. Right ventricular dysfunction in septic shock: assessment by measurements of right ventricular ejection fraction using the thermodilution technique. Acta Anaesthesiol Scand. 1989;33(1):34–8. https://doi.org/10.1111/j.1399-6576.1989.tb02856.x.
14. Mertens LL, Friedberg MK. Imaging the right ventricle--current state of the art. Nat Rev Cardiol. 2010;7(10):551–63. https://doi.org/10.1038/nrcardio.2010.118.
15. Oe M, Gorcsan J, Mandarino WA, Kawai A, Griffith BP, Kormos RL. Automated echocardiographic measures of right ventricular area as an index of volume and end-systolic pressure-area relations to assess right ventricular function. Circulation. 1995;92(4):1026–33. https://doi.org/10.1161/01.CIR.92.4.1026.
16. Tei C, Dujardin K, Hodge D. Doppler index combining systolic and diastolic myocardial performance: clinical value in cardiac amyloidisis. J Am Coll Cardiol. 1996;28(3):658–64.
17. Sandoval J, Bauerle O, Palomar A, et al. Survival in primary pulmonary hypertension. Validation of a prognostic equation. Circulation. 1994;89(4):1733–44. https://doi.org/10.1161/01.CIR.89.4.1733.

18. Voelkel NF, Quaife RA, Leinwand LA, et al. Right ventricular function and failure: report of a National Heart, Lung, and Blood Institute working group on cellular and molecular mechanisms of right heart failure. Circulation. 2006;114(17):1883–91. https://doi.org/10.1161/CIRCULATIONAHA.106.632208.
19. Barst RJ, Gibbs JS, Ghofrani HA, et al. Updated evidence-based treatment algorithm in pulmonary arterial hypertension. J Am Coll Cardiol. 2009;54(1 Suppl):S78–84. https://doi.org/10.1016/j.jacc.2009.04.017.
20. Hassoun PM, Mouthon L, Barberà JA, et al. Inflammation, growth factors, and pulmonary vascular remodeling. J Am Coll Cardiol. 2009;54(1 Suppl):S10–9. https://doi.org/10.1016/j.jacc.2009.04.006.
21. Frantz S, Bauersachs J, Ertl G. Post-infarct remodelling: contribution of wound healing and inflammation. Cardiovasc Res. 2009;81(3):474–81. https://doi.org/10.1093/cvr/cvn292.
22. Wauthy P, Pagnamenta A, Vassalli F, Naeije R, Brimioulle S. Right ventricular adaptation to pulmonary hypertension: an interspecies comparison. Am J Physiol Heart Circ Physiol. 2004;286(4):H1441–7. https://doi.org/10.1152/ajpheart.00640.2003.
23. Grignola JC, Ginés F, Bia D, Armentano R. Improved right ventricular-vascular coupling during active pulmonary hypertension. Int J Cardiol. 2007;115(2):171–82. https://doi.org/10.1016/j.ijcard.2006.03.007.
24. Ghuysen A, Lambermont B, Kolh P, et al. Alteration of right ventricular-pulmonary vascular coupling in a porcine model of progressive pressure overloading. Shock. 2008;29(2):197–204. https://doi.org/10.1097/SHK.0b013e318070c790.
25. Missant C, Rex S, Segers P, Wouters PF. Levosimendan improves right ventriculovascular coupling in a porcine model of right ventricular dysfunction. Crit Care Med. 2007;35(3):707–15.
26. Burkhoff D, Mirsky I, Suga H. Assessment of systolic and diastolic ventricular properties via pressure-volume analysis: a guide for clinical, translational, and basic researchers. Am J Physiol Heart Circ Physiol. 2005;289(2):H501–12. https://doi.org/10.1152/ajpheart.00138.2005.
27. Kelly RP, Ting C, Yang T, et al. Effective arterial elastance as index of arterial vascular load in humans. Circulation. 1992;86:513–21. https://doi.org/10.1161/01.CIR.86.2.513.
28. Lam CSP, Roger VL, Rodeheffer RJ, et al. Cardiac structure and ventricular-vascular function in persons with heart failure and preserved ejection fraction from Olmsted County, Minnesota. Circulation. 2007;115(15):1982–90. https://doi.org/10.1161/CIRCULATIONAHA.106.659763.
29. Sanz J, García-Alvarez A, Fernández-Friera L, et al. Right ventriculo-arterial coupling in pulmonary hypertension: a magnetic resonance study. Heart. 2012;98(3):238–43. https://doi.org/10.1136/heartjnl-2011-300462.
30. Trip P, Kind T, van de Veerdonk MC, et al. Accurate assessment of load-independent right ventricular systolic function in patients with pulmonary hypertension. J Heart Lung Transplant. 2013;32(1):50–5. https://doi.org/10.1016/j.healun.2012.09.022.
31. Alyono D, Larson VE, Anderson RW. Defining end systole for end-systolic pressure-volume ratio. J Surg Res. 1985;39(4):344–50. https://doi.org/10.1016/0022-4804(85)90113-1.
32. Sato T, Tsujino I, Oyama-Manabe N, et al. Simple prediction of right ventricular ejection fraction using tricuspid annular plane systolic excursion in pulmonary hypertension. Int J Card Imaging. 2013;29(8):1799–805. https://doi.org/10.1007/s10554-013-0286-7.
33. Ogihara Y, Yamada N, Dohi K, et al. Utility of right ventricular Tei-index for assessing disease severity and determining response to treatment in patients with pulmonary arterial hypertension. J Cardiol. 2013. http://www.sciencedirect.com/science/article/pii/S0914508713002220. Accessed 16 Sept 2013.
34. Badesch DB, Champion HC, Sanchez MAG, et al. Diagnosis and assessment of pulmonary arterial hypertension. J Am Coll Cardiol. 2009;54(1 Suppl):S55–66. https://doi.org/10.1016/j.jacc.2009.04.011.
35. Zhang Y, Wang Y, Wang W, Liu B. Doppler ultrasound signal denoising based on wavelet frames. IEEE Trans Ultrason Ferroelectr Freq Control. 2001;48(3):709–16.
36. Tei C, Nishimura RA, Seward JB, Tajik AJ. Noninvasive Doppler-derived myocardial performance index: Correlation with simultaneous measurements of cardiac catheterization measurements. J Am Soc Echocardiogr. 1997;10(2):169–78. https://doi.org/10.1016/S0894-7317(97)70090-7.
37. Monroe RG, French GN. Left ventricular pressure-volume relationships and myocardial oxygen consumption in the isolated heart. Circ Res. 1961;9(2):362–73. Available from: http://circres.ahajournals.org/cgi/doi/10.1161/01.RES.9.2.362
38. Monroe RG, French G. Ventricular pressure-volume relationships and oxygen consumption in fibrillation and arrest. Circ Res. 1960;8(1):260–6. Available from: http://circres.ahajournals.org/cgi/doi/10.1161/01.RES.8.1.260
39. Monroe RG, Strang RH, LaFarge CG, Levy J. Ventricular performance, pressure-volume relationships, and O2 consumption during hypothermia. Am J Physiol. 1964;206(1):67–73.
40. Lafontant R, Feinberg H, Katz L. Pressure-volume relationships in right ventricle. Circ Res. 1962;11:699–701. Available from: http://circres.ahajournals.org/content/11/4/699.short
41. Taylor R, Covell J, Ross J Jr. Volume-tension diagrams of ejecting and isovolumic contractions in left ventricle. Am J Physiol. 1969;216:1097–102. http://ajplegacy.physiology.org/content/ajplegacy/216/5/1097.full.pdf
42. Cross C, Rieben P. Influence of coronary perfusion and myocarckd edema on pressure-volume diagram of left ventricle. Am J Physiol. 1961;201:102–8. Available from: http://ajplegacy.physiology.org/content/ajplegacy/201/1/102.full.pdf

43. Hild R, Mechelke K, Nusser E. Über die Beziehungen zwischen dem Druck und der Stromstärke in der Arteria pulmonalis sowie der Leistung des rechten Ventrikels beim "unbeeinflußten Kreislauf" der Katze und im oligämischen Schock. Pflüger's Archiv für die gesamte Physiologie des Menschen und der Tiere. 1956;263(4):401–10. Available from: http://link.springer.com/article/10.1007/BF00380426
44. Hild R, Sick L. Das Druck-Volumen-Diagramm des isolierten spontan schlagenden Katzenherzens. Z Biol. 1955;107:51. Available from http://scholar.google.com/scholar?q=hild+and+sick+1955&btnG=&hl=en&as_sdt=0%2C6#1
45. Ullrich KJ, Riecker G, Kramer K. Das Druckvolumdiagramm des Warmbl terherzens. Pflügers Arch for die Gesamte Physiol des Menschen und der Tiere. 1954;259(6):481–98. Available from: http://link.springer.com/10.1007/BF00412913